Low-cost Posidonia oceanica bio-adsorbent for efficient removal of antibiotic oxytetracycline from water

Karima Ferchichi, Noureddine Amdouni, Yves Chevalier, Souhaira Hbaieb

Low-Cost Posidonia Oceanica Bio-adsorbent for Efficient Removal of Antibiotic Oxytetracycline from Water

Karima Ferchichi[1], Noureddine Amdouni[1], Yves Chevalier[2], Souhaira Hbaieb[1]*

1- *Laboratoire de Recherche: Caractérisations, Applications et Modélisation de Matériaux, Université de Tunis El Manar, Faculté des Sciences de Tunis, Campus universitaire El Manar, Tunisia.*
2- *Laboratoire d'Automatique, de Génie des Procédés et de Génie Pharmaceutique, Université de Lyon 1, UMR 5007 CNRS, 43 bd 11 Novembre, 69622 Villeurbanne, France.*

* Corresponding authors: Souhaira Hbaieb: E-mail: souhaira.hbaieb@fst.utm.tn

Tel: +216 98 94 74 79 Fax: +216 71 53 76 88

Abstract. The presence of antibiotics as micro-contaminants in the water and aqueous environments is a health concern to humans and the ecosystem. Therefore, their elimination by adsorption to available and cheap materials in water treatment plants is a research topic of high relevance. The present paper reports on the adsorption behavior of Oxytetracycline on a bio-adsorbent prepared from Posidonia Oceanica; an abundant Mediterranean biomass. Characterization of the pretreated Posidonia biomaterial was achieved using several analyses such as Boehm acid–base titration method, pH_{PZC} determination and analysis techniques (FTIR, ^{13}C CP-MAS NMR, optical microscopy and TGA). The pH_{PZC} occurred around pH 2.11. Posidonia biomaterial showed a fast and high uptake rate throughout the adsorption process, which is a definite advantage for analytical applications such as water decontamination. The experimental kinetic data fitted very rightly the pseudo-second-order kinetic model and the equilibrium uptake can adopt the bi-Langmuir isotherm model for all studied pH values which assumes adsorptions at the two localized sites. Maximum adsorption capacities of 11.8 $mg{\cdot}g^{-1}$ and 4.4 $mg{\cdot}g^{-1}$ for the two adsorption sites are reached at pH 6. The oxytetracycline adsorption process onto Posidonia bio-adsorbent is spontaneous ($\Delta_{ads}G^0 < 0$), exothermic ($\Delta_{ads}H^0 < 0$), and entropically favorable ($\Delta_{ads}S^0 > 0$). The effect of pH on adsorption behavior and the thermodynamic parameters of adsorption are consistent with a possible origin of adsorption of Oxytetracycline by means of hydrogen bonding interactions between surface hydroxyl and phenolic groups of the biomaterial and Oxytetracycline. The proposed green and environmentally friendly biomaterial offers potential benefits as a bio-adsorbent in the remediation of aquatic environments contaminated by various organic materials.

Keywords: Posidonia biomaterial, Antibiotic removal, Adsorption, Bi-Langmuir isotherm model, Thermodynamic parameters.

1. Introduction

Oxytetracycline (OTC) is an antibiotic applied for the treatment of bacterial infections in humans and animals (Ma et al. 2016). Curative and preventive treatments of bacterial infections improve the production of farm animals; this is the reasons why OTC is widely used in animal husbandry such as aquaculture and livestock (Lu et al. 2021; Qin et al. 2022). The use of OTC in dairy cows is beneficial to farmers, which has improved production performance. However, this antibiotic is a chemical that persists for a long time in the animal tissues and in the environment. It finally accumulates in the environment, especially in water, which can lead to the spread of antibiotic resistance genes and disrupt the functioning of the ecosystem (Zhao et al. 2020). The development of resistant species that can be extracted in bovine milk is considered a significant source of toxicological harmful effects to consumers such as allergic reactions, liver damage, tooth yellowing, and gastrointestinal disturbance (Liu et al. 2018). To protect humans from exposure to these drug residues present in water, there is a need for effective and robust methods to separate micro-pollutants from contaminated water. In this respect, very different technologies for antibiotic removal from contaminated water are reported (Cheng et al. 2021, De Leon-Condes et al. 2017, Fanourakis et al. 2020, Ribeiro et al. 2018) including electrochemical oxidation (Dos Santos et al. 2021, Rahmani et al. 2018), photocatalytic degradation (Chenguang et al. 2022), ultrafiltration (Hembach et al. 2019) and chemical precipitation (Saleh et al. 2022). However, such techniques have several limitations pertaining to their cost, efficiency, design and durability. The most widely used method relies on adsorption, which is of high efficiency and low operating costs (Banhishikha et al. 2020, Dutta and Mala 2020, Geetha et al. 2020). The conventional adsorbent made of modified silica (Ayadi et al. 2019, Zeidman et al. 2020) is a rather expensive material (Ayadi et al. 2020, Han et al. 2022). Alternative low-cost adsorbents derived from natural materials, industrial and agricultural solid wastes have been proposed in recent investigations (Gupta et al. 2021). Indeed, adsorption using biomass materials has been demonstrated to be one of the easiest and most efficient ways to uptake and retain various contaminants from contaminated matrices (De Gisi et al. 2016). For example, a few studies aiming at fixing such issues, put forward the use of biochar as a low-cost adsorbent material (Wang et al. 2018). As instances, virgin softwood biochar was used as an adsorbent medium to remove dissolved arsenic from contaminated groundwater (Boni et al. 2021); and rambutan peel waste hydrochar was applied as an adsorbent to remove Fe(II) contaminants from aqueous media (Normah et al. 2022). Several research studies have also indicated that certain methods can be used to remove recalcitrant contaminants such as carbamazepine from water by adsorption onto granular activated carbon and biological activated carbon (Décima et al. 2021). Additionally, technologies incorporating the modification of biochar have been reported to improve their sorption capacity for

various chemical contaminants. For instance, modified coal fly has much higher sorption ability to acid and reactive dyes than carbon black or chitosan (Hussain et al. 2022). The present study aims at investigating the feasibility and potential benefits of introducing marine seagrass balls as a bio-adsorbent. Posidonia Oceanica (L.) Delile, from the Posidoniaceae family and commonly known as Neptune grass or Mediterranean tapeweed, a native biomass abundant on the coasts of Tunisia, has demonstrated its ability to remove both organic and inorganic molecules (Ben Douissa et al. 2016; Boubakri et al. 2017; Elmorsi et al. 2019). The main constituents of Posidonia Oceanica balls are cellulosic substances (cellulose and hemicellulose, 62%) together with a relatively high content of lignin (27%) (Maisano et al. 2019). Herein, we have developed efficient bio-adsorbent materials using Posidonia Oceanica balls to extract OTC antibiotics from water. This topic has previously been addressed in an investigation of the adsorption of tetracycline antibiotic onto Posidonia bio-adsorbent focusing on the relationships between the processing parameters and the adsorption behavior using a neural network approach (Donut and Cavas 2017). The present work addresses the characterization of the Posidonia bio-adsorbent and physicochemical mechanisms of OTC adsorption through a thermodynamic study. The kinetics of adsorption was assessed as it is of high relevance with regards to water treatment process.

2. Materials and Methods

2.1. Reagents and chemicals

Oxytetracycline (OTC) was supplied by Sigma-Aldrich. All chemicals and solvents used were of analytical grade. All solutions were made with Milli-Q water of 18 MΩ·cm resistivity.

2.2. Characterization methods

IR spectra were recorded with a Bruker IFS 55 Equinox FTIR spectrometer in ATR mode. CP MAS ^{13}C NMR spectra of Posidonia biomaterials were run on a Bruker Avance III 500 ultra-shield PLUS spectrometer. The thermal stability of all the prepared Posidonia biomaterials was studied by thermogravimetric analyses (TGA) carried out on a TG209F1 Netzsch instrument. The analysis was performed in the temperature range of 25–1000 °C at a rate of 10°C·min^{-1} under a dynamic atmosphere of nitrogen. Zeta potentials were measured by electrophoresis with Malvern Zetasizer Nano ZS, with 0.05 wt% aqueous suspensions at different pH values. The ζ potential was calculated from the electrophoretic mobility under the Smoluchowski approximation. The ultraviolet-visible (UV–vis) spectrophotometer (Varian Cary 50 type) was employed for the measurement of absorbance of OTC solutions. Optical microscopy pictures of Posidonia biomaterials dispersions were taken with a Leica DMLM microscope.

A drop of the aqueous dispersion was observed in transmission mode between glass slide and cover slip at magnifications of the objective ranging from ×10 to ×100.

2.3. Preparation of Posidonia biomaterials

Posidonia Oceanica balls were collected from the Cheba-Mahdia beach at the east coast of Tunisia. The fibers of biomass balls have been manually separated, extensively washed with large volumes of distilled water to remove sand and salt coming from sea water, and then dried in the open air. The obtained Posidonia fibers were washed in a Soxhlet extractor with ethanol during 24 h and dried in an oven at 50 °C for 48 h, until the mass of the fibers stayed constant. The dry biomass materials were crushed, sieved in order to recover particles of homogeneous size (100, 75 and 50 μm), washed several times with distilled water, and oven dried for 24 h at 50–60 °C. After that, the fibers and crushed Posidonia were stored in a desiccator for further use. The prepared fiber and powder materials and the corresponding abbreviations as used throughout the paper are listed in Table 1.

Table 1. List of the studied materials with their abbreviations.

Bio-materials	**Abbreviations**
Posidonia fiber	POS-fiber
Posidonia powder (medium width 100 μm)	POS-100
Posidonia powder (medium width 75 μm)	POS-75
Posidonia powder (medium width 50 μm)	POS-50

2.4. Characterization of raw materials

The elemental and moisture content analysis of dry Posidonia Oceanica fibers were determined. Elemental content of carbon, sulfur, nitrogen and hydrogen were determined using a Perkin Elmer type series II analyzer 2400. Posidonia Oceanica raw material has contents of C = 43.65%, S = 2.73%, N = 1.19% and H = 6.12%, which are similar to those previously reported in case of other Posidonia raw materials (Zaafouria et al. 2016). The percentage moisture content was calculated by the difference between wet mass and dry mass of 2 g of Posidonia fibers using a muffle oven at 105 °C until the mass of dried matter became constant. The moisture content was 9.53%.

2.5. Surface characterization of Posidonia functional groups

Acidic functions of POS-50 were characterized by acid–base titrations using the Boehm method (Boehm 2002). First, aqueous solutions of $NaHCO_3$ (0.02 mol·L^{-1}), Na_2CO_3 (0.02 mol·L^{-1}) and NaOH (0.02 mol·L^{-1}) were freshly prepared. Then, 0.3 g of POS-50 was added to 20 mL of each base prepared solution. The samples were stirred for 24 h (400 rpm, room temperature), centrifuged and the base excess was titrated with 0.02 M HCl. The amount of acidic groups on the POS-50 surface particle was calculated on the assumptions that: NaOH neutralizes carboxylic, lactonic, and phenolic groups, Na_2CO_3 neutralizes carboxylic and lactonic groups and $NaHCO_3$ neutralizes only

carboxylic groups. The number of surface basic sites was calculated from the amount of HCl that reacted with the deprotonated functional surface of POS-50. The titrations were repeated three times.

2.6. Binding experiments

2.6.1. Calibration curve of UV–vis absorbance

The concentrations of OTC standard solutions were prepared by appropriate dilution in water of the mother solution at 10^{-4} mol·L^{-1} stored at 4 °C. The concentrations of the solutions ranged between 175 and 20 µmol·L^{-1}. Their absorbance at 352 nm wavelength was linear with respect to the concentration.

2.6.2. Effect of adsorbent mass

The tests were conducted by stirring 10 mL of 80 mg L^{-1} OTC solutions, with different masses of Posidonia biomaterials (POS-50, POS-75, POS-100 and POS-fiber) at 25 °C and pH 6.0. The mixture of each sample was centrifuged and the residual concentration of OTC in the supernatant was determined by absorbance measurements at the appropriate wavelength (λ_{max} = 352 nm).

2.6.3. Adsorption experiments

All adsorption measurements were performed by the depletion method in water since real environmental samples were essentially aqueous media. For equilibrium adsorption, the biomaterial (80 mg) was immersed in 10 mL of water containing OTC with various concentrations ranging from 20 to 175 µmol·L^{-1} and shaken at 380 rpm constant shaking rate at constant temperature in thermostatic water bath. The initial pH of both OTC solutions and Posidonia materials was maintained at a fixed value 2, 4.5, 6 or 8 using 1 M HCl or 0.1 M NaOH solutions. The mixtures were stirred for different contact times *t*, and then centrifuged at 5000 rpm for 10 min. The residual concentration of OTC (*Ce*, mol·L^{-1}) in the supernatant was determined by UV–vis absorbance analysis (λ_{max} = 352 nm).

The dynamic adsorption capacities (*Qe*, mol·g^{-1}) and adsorption percentage (%A, %) of OTC were calculated according to the following equations.

$$Qe = \frac{V}{m}(C_0 - Ce) \quad \text{(Eq 1)}$$

$$\%A = (C_0 - Ce)\frac{100}{C_0} \quad \text{(Eq 2)}$$

where C_0 and *Ce* respectively are the initial and the residual concentrations of OTC, *V* is the volume of the OTC solution, *m* is the mass of Posidonia biomaterials. The experiments were performed at 298 K unless otherwise indicated.

3. Results and discussion

3.1. Physicochemical characterization of Posidonia

The contents of carbon, hydrogen, nitrogen and sulfur, the surface functional characterization and point of zero charge of POS-50 are given in Table 2. According to such analyses, the major elements of POS-50 were carbon and hydrogen, which are the basic elements of cellulose, hemicellulose and lignin (Meseguer et al. 2016). The percentage of carbon and hydrogen were similar to those previously observed in the case of other cellulosic materials such as, cherry stones (Nowicki et al. 2015), olive seed (Stavropoulos and Zabaniotou 2005) and vetiver roots (Gaspard et al. 2007), which have elemental contents of C = 46–49% and H = 5.7–6.0%. The Boehm titration method was applied to identify and quantify the surface functions of POS-50. They are split into three types: acidic, basic, or neutral. The main acidic groups on Posidonia surface are carboxylic, lactonic and phenolic groups (Pennesi et al. 2013, Astudillo-Pascual et al. 2021). The heterogeneous POS-50 has a wide variety of functional surface groups that may act as adsorption sites for OTC adsorption. Table 2 summarizes the experimental surface functions determined by Boehm titration of POS-50. The surface composition of Posidonia mostly included carboxylic acidic functional groups, followed by phenolic and then lactonic groups that are the main acidic functions of lignin and hemicelluloses contained in Posidonia (Douissa et al. 2013).

Table 2. pH_{PZC} value and Boehm titration results of POS-50.

pH_{PZC}	**Elemental composition (%)**				**Surface functional groups (mmol g^{-1})**		
2.11	C	H	N	S	Carboxylic	Phenolic	Lactonic
	39.75	5.57	0.91	2.53	0.797	0.127	0.009

Infrared spectra of POS-50, POS-75, POS-100 and POS-fiber were collected in the wavenumber range 400–4000 cm^{-1} (Fig. 1). All biomaterials presented similar spectra. The functional groups present on the bio-adsorbent surface are essential for understanding the adsorption mechanism. The main absorption bands observed in the IR spectrum of POS-50 were those of cellulose, hemicellulose and lignin, which are characterized by the presence of carbonyl, hydroxyl and methoxy functional groups. The broad band in the range 3700–3000 cm^{-1} (with maximum absorption at 3334 cm^{-1}) showed the existence of –OH and –NH vibrations (Tarchoun et al. 2019). The two small bands located at 2971 and 2886 cm^{-1} are due to asymmetric and symmetrical C–H stretching vibrations attributed to alkyl groups respectively. The band at 1617 cm^{-1} was assigned to amide $C(O)NH_2$ bond and the one at 1425 cm^{-1} corresponded to the deformation vibration of –C–OH with contribution from the symmetrical stretching vibration O–C–O of the carboxylate group (Radhakrishnan et al. 2021). Particularly, this band at 1425 cm^{-1} is also known as the crystalline band. The band located at 1254 cm^{-1} was attributed to the O–C–O segment of the ester group. Finally, the band at 1019 cm^{-1} was assigned to alcoholic groups (El Achaby et al. 2018).

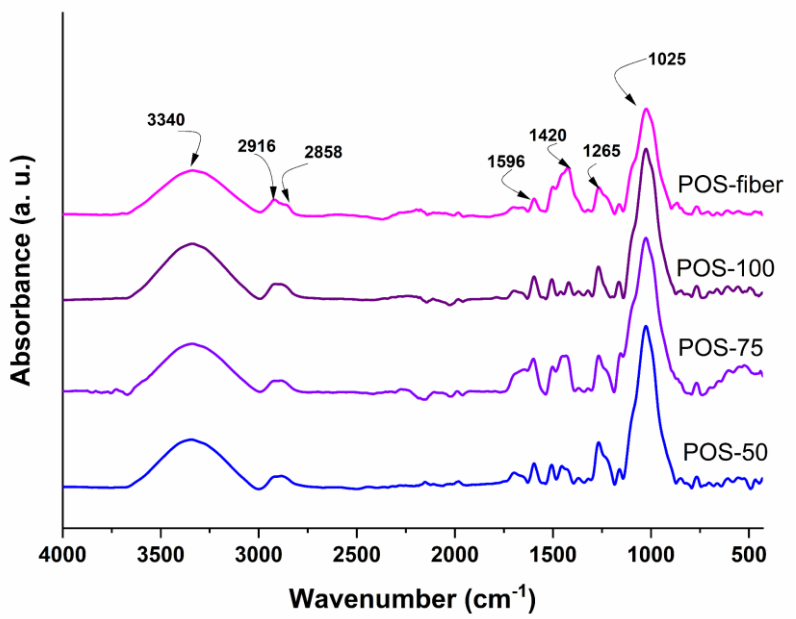

Figure 1. FTIR spectra of POS-50, POS-75, POS-100 and POS-fiber biomaterials.

CP MAS ^{13}C NMR spectroscopy is the most effective method for the characterization of the lignocellulosic materials and is able to provide detailed information directly on the solid sample. The solid-state ^{13}C NMR spectrum of the POS-50 bio-adsorbent (Fig. 2) exhibited strong signals in the range 20–190 ppm mainly corresponding to the different carbons of cellulose, hemicellulose and lignin moieties. The strong signals in the region between 50 and 107 ppm were assigned to the different carbons of cellulose and hemicelluloses (Chadlia and Farouk 2010). NMR technique allows differentiating the crystalline and paracrystalline domains since the carbons located inside the crystalline regions have a distinct chemical shift from the carbons located on the crystal surfaces or inside the paracrystalline domains. Cellulose consists of crystalline and non-crystalline phases in different ratios, depending on the natural source. The crystallinity index (Cr.I.) of cellulose can be calculated from the ^{13}C CP MAS NMR spectra by integrating the C_4 signals at 84–93 ppm for crystalline cellulose and at 79–84 ppm for amorphous cellulose (Coletti et al. 2013). According to the spectrum shown in Fig. 2, the Cr.I. value of POS-50 is 41%. In the crystalline phase, the cellulose fibers are ordered by inter- and intramolecular hydrogen bonds, on the other hand in the non-crystalline phase, the network does not have an organized structure (Wohlert et al. 2022). The only signal that could be assigned to lignin was that belonging to the methoxy group of the aromatic moieties at 56 ppm. In addition, the region between 106 and 180 ppm was specific for the aromatic carbons of lignin.

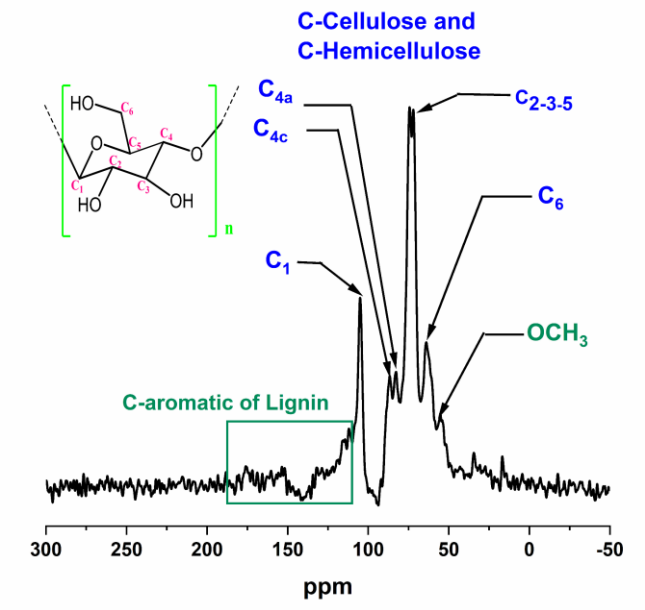

Figure 2. ^{13}C CP MAS NMR spectrum of POS-50.

The investigation of the thermal properties of Posidonia biomaterials is essential for its applications. The TGA curves of POS-fiber, POS-100, POS-75 and POS-50 are shown in Fig. 3. Table 3 reports the results of thermal analyses. The degradation process of these biomaterials took place in three stages. The first mass loss in the temperature range of approximately 20 to 150 °C was caused by the evaporation of moisture (Tarchoun at al. 2019). The second mass loss in the range 230–360 °C was attributed to the preponderant process of decomposition of the carbohydrate phase of Posidonia made of hemicellulose (the most thermally unstable compound) and cellulose (e.g. dehydration, depolymerization, decarboxylation, and decomposition of glycosyl units). The third stage appearing in the range 375–1000 °C corresponded to char combustion and the inorganic-mineral decomposition (Haddar et al. 2018). According to the results described in previous reports (Plis et al. 2016), the main gases produced during the process and detected by MS and FTIR spectrometers are CH_4, CO, H_2O, light hydrocarbons (C_2H_4, C_2H_6, C_3H_6) and CO_2. These gases reach their maximum yields in the temperature range of 230 to 530 °C. At higher temperatures, all gases are oxidized to CO_2 (Plis et al. 2014). It is clear that the thermal behavior of the Posidonia is improved by decreasing its size throughout the temperature range studied. Indeed, the kinetics of degradation were slower for smaller sizes.

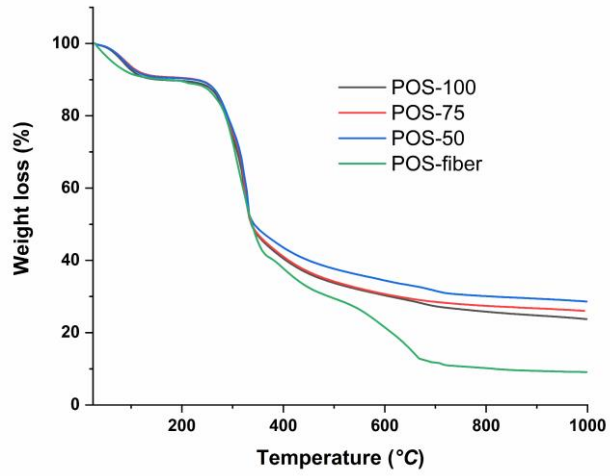

Figure 3. Thermogravimetric analysis of POS-50, POS-75, POS-100 and POS-fiber biomaterials.

Table 3. Mass losses from TGA of POS-50, POS-75, POS-100 and POS-fiber biomaterials.

Bio-materials	1st mass loss (%) (20–150 °C)	2nd mass loss (%) (230–360 °C)	3rd mass loss (%) (375–1000 °C)
POS-fiber	10.0	49.3	31.8
POS-100	10.0	44.8	21.5
POS-75	9.2	45.2	19.4
POS-50	9.4	43.3	18.8

The adsorption of OTC was studied by the depletion method. Ionization behaviors have a significant influence on the adsorption of OTC on bio-adsorbents. Indeed, the OTC is a complex organic compound having particular chemical characteristics and behaviors with several ionizable functional groups. Oxytetracycline has three pK_a and hence can exist as cationic, zwitterionic or anionic species, under acidic, neutral and alkaline conditions, they respectively (Prarat et al. 2020), as show in Fig. 4. OTC adsorption to Posidonia biomaterial and other sorbents is expected to be considerably influenced by its ionization behavior (Aghababaei et al. 2017). Aqueous speciation of OTC was also considered following the reactions below:

$$OTC_T \leftrightarrows OTCH_3^+ + OTCH_2^0 + OTCH^- + OTC^{2-} \quad \text{(Eq 3)}$$

$$OTCH_3^+ \leftrightarrows OTCH_2^0 + H^+ \quad \text{(Eq 4)}$$

$$OTCH_2^0 \leftrightarrows OTCH^- + H^+ \quad \text{(Eq 5)}$$

$$OTCH^- \leftrightarrows OTC^{2-} + H^+ \quad \text{(Eq 6)}$$

The OTC_T in the reactions represents all possible solutions species for OTC. The pK_a values (Fig. 4) were taken from the literature (Punamiya et al. 2013).

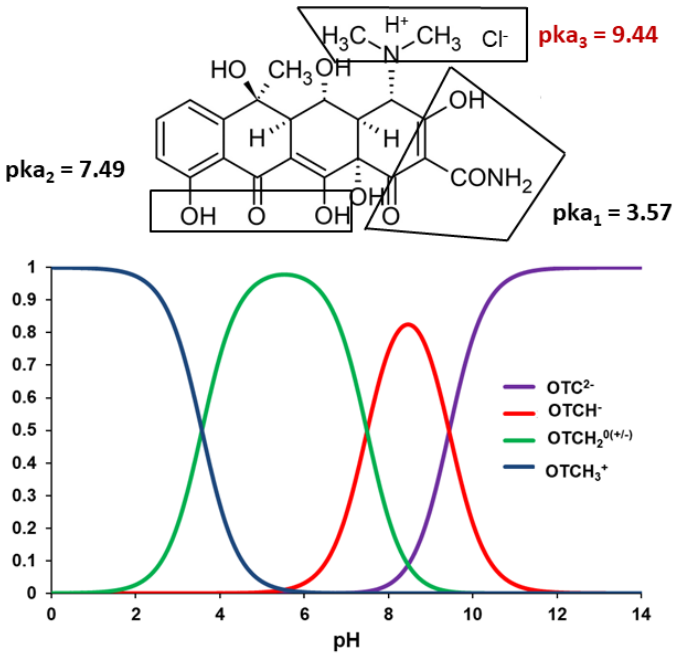

Figure 4. Structure and pH-dependent surface speciation of oxytetracycline. The fractions of each ionic species are calculated using the log(*K*a) values of OTC, where $OTCH_3^+$, $OTCH_2^0$ (±), $OTCH^-$, and OTC^{2-} represent the different ionic species of OTC.

The pH is a very important parameter in the adsorption process because it strongly influences the surface charge of the adsorbent and the ionic form of the adsorbates (Fig. 5), which both affect the adsorption behavior. To elucidate the role of surface charge of the adsorbent in the adsorption of OTC molecules, the point of zero charge (pH_{PZC}) of Posidonia was determined. This corresponds to the pH value of the medium for which the positive and negative charges are balanced, so that the overall surface charge is zero. The pH_{PZC} is important in adsorption phenomena, especially when electrostatic interactions are involved, which presently is the case. It was determined by zeta potential measurements in aqueous suspension of POS-50 of variable pH values between 2 and 10 set by the addition of 0.1 M NaOH or HCl solution. The suspensions must be kept under constant agitation at ambient temperature for 4 h to equilibrate the final pH. The pH_{PZC} of POS-50 was close to pH 2 (Fig. 5). Therefore, the overall surface charge was negative above pH 2. This result was expected since the POS-50 material mostly contains polar functions such as phenolic and carboxylic groups whose ionization yields negatively charged groups. Upon increasing the pH, the zeta-potential decreased from −2 mV to −18 mV at pH 10.

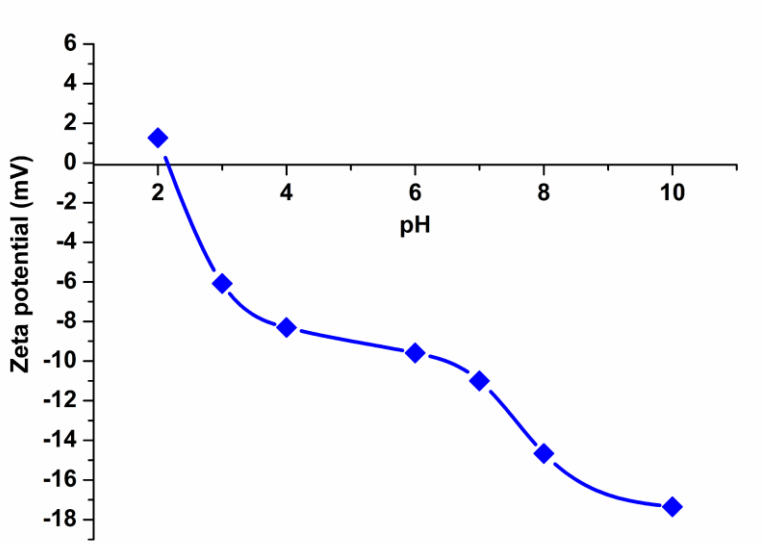

Figure 5. Zeta potential measurements of POS-50 at different pH.

Different dispersions of POS-50, POS-75, POS-100 and POS-fiber in water were observed with optical microscopy (Fig. 6). The dimensions of the observed pieces of fibers depended on the type of mechanical crushing and sieving processes. All the materials kept their fiber morphology under mechanical grinding; just the fiber sizes were modified. All materials showed individualized fibers with regular shape, clear and smooth surface. The approximate fiber lengths of individualized POS-50, POS-75, POS-100 and POS-fiber were 3, 8, 10 and 110 μm respectively.

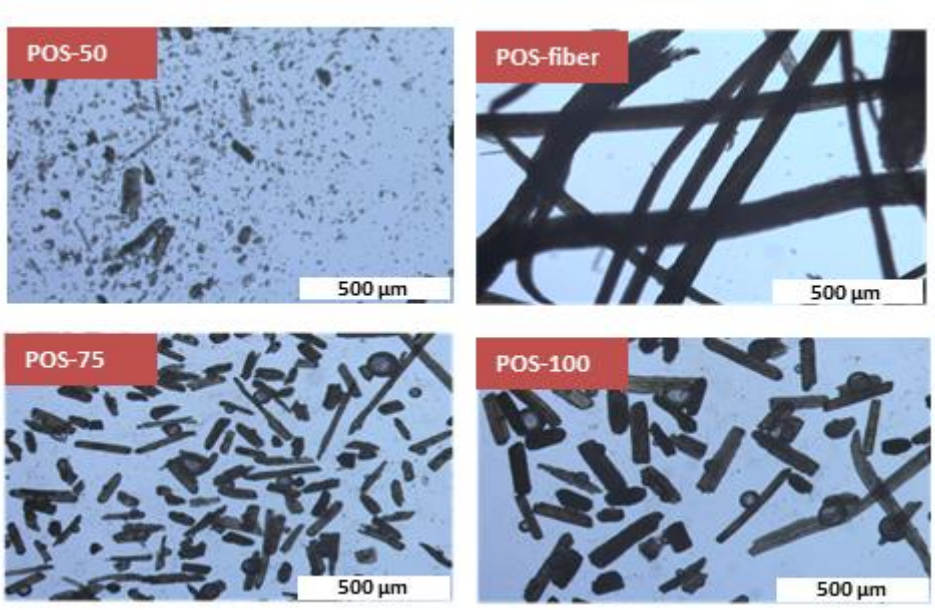

Figure 6. Optical microscopy pictures of POS-50, POS-75, POS-100 and POS-fiber in water under magnification (×20).

3.2. Performance for adsorption of oxytetracycline

3.2.1. Effect of adsorbent type and mass

The influence of adsorbent mass has been studied in the range 0.020–0.100 g. The histogram in Fig. 7 shows that POS-50 was more efficient at adsorbing OTC and that maximum adsorption of 86% was reached for the masses of POS-50 of 0.08 g and above. The efficiency of POS-50 was significantly higher than other samples that could uptake a maximum of OTC antibiotics in the range 45–75%. This optimum mass of POS-50 corresponds to the specific conditions of this series of experiments with a fixed OTC concentration of 80 mg L^{-1} and a volume of aqueous solution of 10 mL. The amount of adsorbent dispersed in the solution is to be set with regards to the amount of OTC molecules to be uptaken so as to ensure an equivalent number of adsorption sites. Beyond a certain mass of bio-adsorbent, the adsorption rate slightly decreased, indicating that supplementary phenomena detrimental to adsorption were operating. A possible origin of this phenomenon is the poor dispersion of POS-50 at too high concentrations. Indeed, aggregation of Posidonia fibers lowers the accessibility to the fibers surface and prevents OTC from reaching adsorption sites. Therefore, there is an optimum concentration of bio-adsorbent, which avoids such an ineffective overdose. In the further study aiming at determining the adsorption capacities by saturating all sites, adsorbent masses of 0.08 g of POS-50 were chosen.

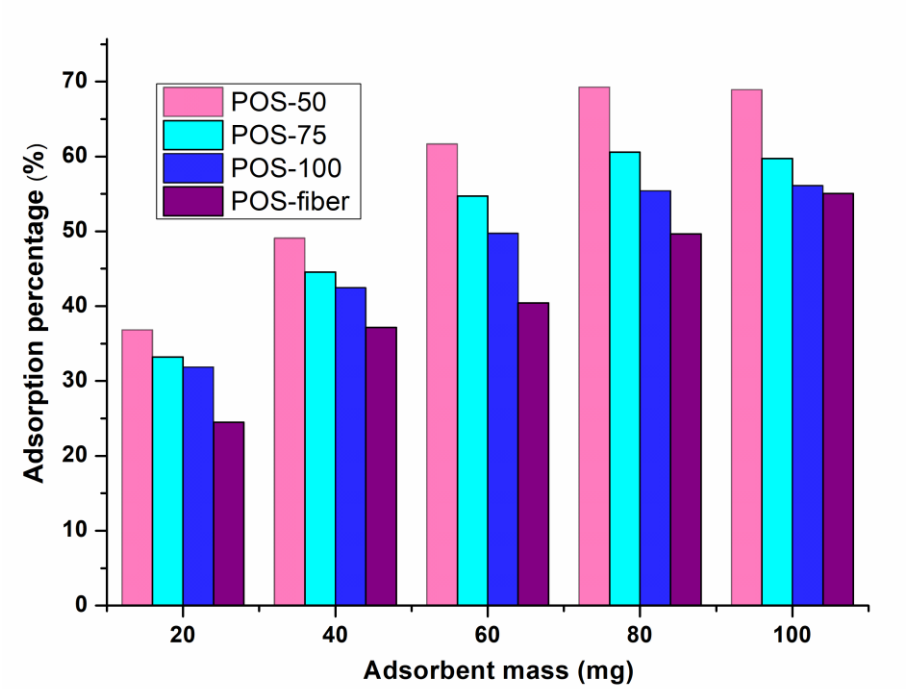

Figure 7. Effect of the mass of Posidonia biomaterials on adsorption of OTC from its aqueous solution. Solution volume = 10 mL; Concentration = 80 mg·L^{-1}; contact time = 20 min; and temperature = 298 K.

3.2.2. Effect of pH on oxytetracycline adsorption

Adsorption isotherms represent the thermodynamic equilibrium between adsorbed and free OTC molecules. They have been measured for adsorption to POS-50 after an equilibration time of 20 min. The bi-Langmuir theoretical adsorption model was fitted to the experimental data to infer the adsorption parameters of OTC onto POS-50 biomaterial at different pH. The most commonly used model of adsorption is the Langmuir model (Langmuir 1918). The Langmuir theory describes monolayer adsorption of adsorbate molecules on a homogeneous surface having a well-defined density of active sites, all sites being identical and independent (Liu et al. 2019). The bi-Langmuir isotherm model considers the presence of two types of adsorption sites (site 1 and site 2) with different densities and affinities for adsorbing molecules (Fornstedt et al. 2013). This model also assumes, as in the case of the Langmuir model, that adsorptions events are localized at the two well-defined specific sites. The bi-Langmuir model is written as the sum of two Langmuir isotherms for the two types of surface sites:

$$Q_e = Q_{e1} + Q_{e2} = \frac{Q_{max,1} K_{a1} C_e}{1 + K_{a1} C_e} + \frac{Q_{max,2} K_{a2} C_e}{1 + K_{a2} C_e} \quad \text{(Eq 7)}$$

where Q_{e1} and Q_{e2} are the adsorbed quantities at equilibrium on the two types of adsorption sites, $Q_{max,1}$ and $Q_{max,2}$ are the densities of sites 1 and 2, and K_{a1} and K_{a2} are the binding constants of adsorption on site 1 and 2. The density of sites $Q_{max,1}$ and $Q_{max,2}$ are also their maximum adsorption capacity. The units of concentration are mg·L^{-1}, which means that the standard state is an ideal solution of concentration 1 mg·L^{-1}. The variations of

thermodynamic parameters with respect to pH are presented in Fig. 8. It can be seen from Fig. 8 that bi-Langmuir model is suitable for describing the adsorption process of OTC onto POS-50 bio-adsorbent. This result is based by minimizing the average relative error (*ARE*, Eq 8, Table 4) by non-linear regression to experimental data, allowing the determination of the binding constants K_{a1} and K_{a2} and adsorbed amounts at full coverage $Q_{max,1}$ and $Q_{max,2}$ for the two localized sites of adsorption.

$$ARE = \frac{1}{n-p}\sum_{i=1}^{n}\left|\frac{Q_{exp,i}-Q_{calc,i}}{Q_{exp,i}}\right| \quad \text{(Eq 8)}$$

where n is the number of data points and p the number of adjustable parameters.

The excellent fit of the bi-Langmuir adsorption model to the experimental adsorption isotherms of the POS-50 at several pH definitely showed the presence of two types of adsorption sites within the bio-adsorbent, with different affinities toward target compounds. Such dual adsorption is obviously related to the chemical composition of Posidonia containing cellulose, hemicellulose and lignin that are monosaccharides and phenolic materials. The obtained parameters $Q_{1,max}$ and $Q_{2,max}$ for both active sites (Table 4) remained at constant values in acidic and basic media because the number of sites in POS-50 is related to the chemical composition of Posidonia. On the contrary, the values of K_{ai} varied with respect to pH because interactions with OTC depend on the ionic state of functional groups of the adsorption sites. It should be noted that K_{ai} values were higher in slightly acidic media where OTC is under its protonated cationic or neutral forms. In basic medium (pH 8.0), both the Posidonia surface and the OTC molecules are strongly negatively charged. Strong electrostatic repulsions prevent adsorption, which is revealed by the low values of K_{ai} for both types of sites. Electrostatic interactions are favoring adsorption in cases of opposite charges of Posidonia and OTC. Such effect vanishes in acidic medium when the pH reaches the pH_{PZC} of Posidonia at pH 2. The electrostatic binding process is based on a cation exchange of OTC for sodium. Possible higher affinity of OTC than sodium might result from its more hydrophobic nature or hydrogen bonding interactions. The pH dependence of adsorption to sites 1 show such an characteristic effect of electrostatic interactions with a low affinity (small K_{a1}) at pH 2 because of lack of negative charge on Posidonia and at pH 8 because of strong electrostatic repulsions, and maximum affinity at intermediate pH. On the contrary, adsorption to sites 2 does not have such a strong dependence on pH, which reveals a lesser influence of electrostatic phenomena and a larger relative contribution of the types of interactions. Such characteristic pH dependence of K_{ai} values for sites 1 and 2 helps at ascribing the nature of these sites. Sites 1 contain the most acidic functions revealed by the Boehm titration method, namely carboxylic acids. Conversely, sites 2 contain weaker acidic phenolic groups. On this basis, sites 1 are belonging to cellulose and hemicellulose whereas sites 2 are belonging to lignin. The predominant non-electrostatic interactions are presumed of two types: hydrogen bonds between the

hydroxyls of cellulosic materials and carbonyl groups of OTC for sites 1, and π-π stacking interactions between the aromatic rings of lignin and OTC for sites 2. Such assignment of sites 1 to cellulose and sites 2 to lignin is in agreement with the values of the densities of adsorption sites with $Q_{1,max} > Q_{2,max}$. Indeed, Posidonia is richer in cellulosic materials than in lignin.

Table 4. Parameters of the fits of the bi-Langmuir model to experimental adsorption data of oxytetracycline onto POS-50 material at different pH.

pH	$Q_{max,1}$ (µmol·g^{-1})	K_{a1}	log(K_{a1})	$Q_{max,2}$ (µmol·g^{-1})	K_{a2}	log(K_{a2})	*ARE*
2.0	11.2	13147	9.4	4.5	26174	10.1	0.012
4.5	11.5	19444	9.8	4.4	19851	9.8	0.053
6.0	11.8	40156	10.6	4.4	41097	10.6	0.055
8.0	11.0	6843	8.8	4.1	672	6.5	0.045

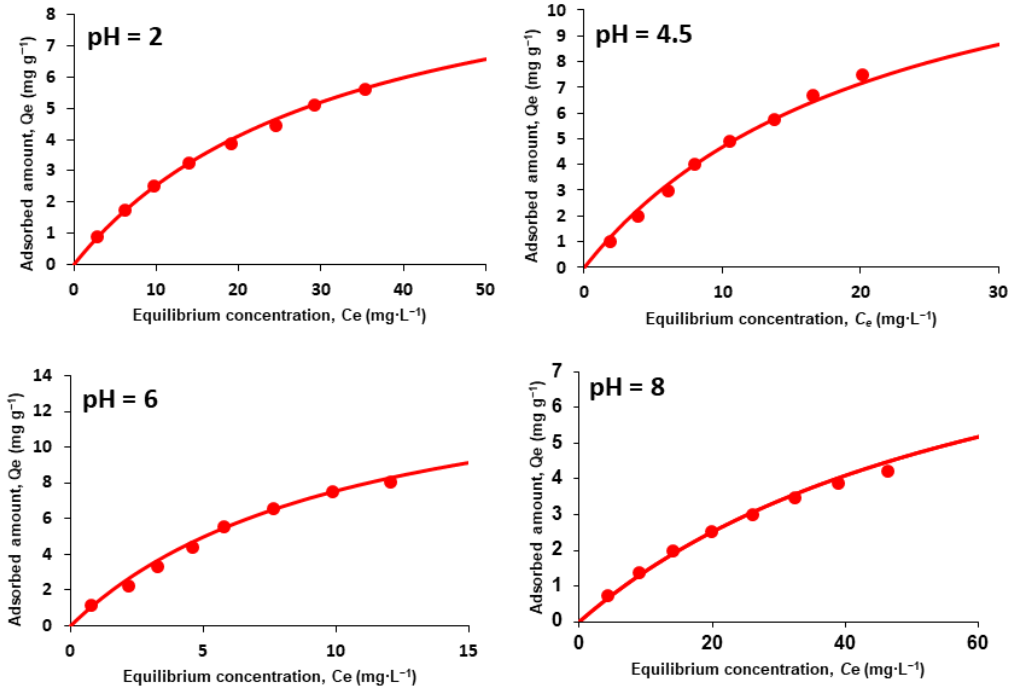

Figure 8. The fit of the bi-Langmuir model to adsorption isotherms of OTC onto POS-50 at various pH at 298 K.

3.2.3. Enthalpic and entropic contributions to the standard free energy of adsorption

The thermodynamic study reflects the feasibility and spontaneous nature of the adsorption process. The thermodynamic parameters of adsorption at pH 6.0 and different temperatures (298 K, 303 K, 313 K and 323 K) such as standard Gibbs free energy $\Delta_{ads}G^0$, standard enthalpy $\Delta_{ads}H^0$ and standard entropy $\Delta_{ads}S^0$ were estimated from $Q_{i,max}$ and K_{ai} parameters from the Gibbs and van't Hoff equations for both binding sites (i = 1 or 2):

$$\Delta_{ads}G_i^0 = -RT\ln(K_{ai}) \quad \text{(Eq 9)}$$

$$\Delta_{ads}G_i^0 = \Delta_{ads}H_i^0 - T\Delta_{ads}S_i^0 \quad \text{(Eq 10)}$$

where R (8.314 J·mol^{-1}·K^{-1}) is the gas constant, T is the absolute temperature, and K_{ai} is the binding constant for either two sites adsorption.

Combination of the two equations gives the van't Hoff equation

$$\ln(K_{ai}) = \frac{\Delta_{ads}S_i^0}{R} - \frac{\Delta_{ads}H_i^0}{RT} \quad \text{(Eq 11)}$$

The van't Hoff plots of ln(Ka_i) against 1/T (Fig. 9a) for the two types of sites were linear with slope $\Delta_{ads}H^0/R$ and y-intercept $\Delta_{ads}S^0/R$. Linear behavior was showing that the values of $\Delta_{ads}H^0$ and $\Delta_{ads}S^0$ did not significantly vary in the studied temperature range (Table 5).

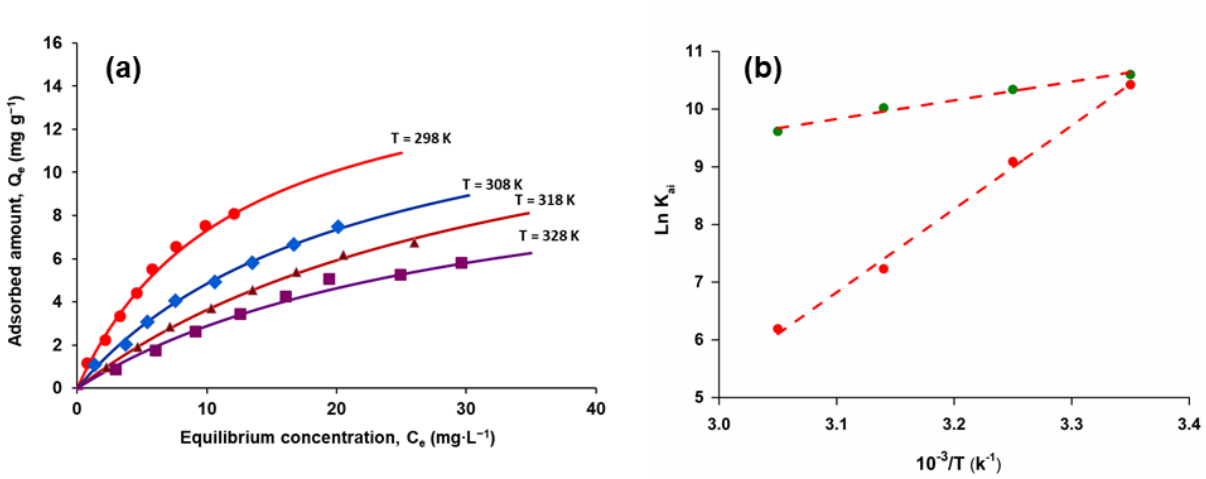

Figure 9. (a): Adsorption isotherms and bi-Langmuir non-linear fit to the adsorption data of OTC onto POS-50 biomaterial at different temperatures. (b): van't Hoff plot of the OTC binding constant onto POS-50 biomaterial against inverse temperature (green dots: site 1 and red dots: site 2).

Table 5. Standard adsorption enthalpy and entropy, $\Delta_{ads}H^0$ and $\Delta_{ads}S^0$, for the two-sites adsorption of OTC to POS-50 at pH 6.0 and $\Delta_{ads}G^0$ at 298 K.

	$\Delta_{ads}H^0$ (kJ·mol^{-1})	$\Delta_{ads}S^0$ (J·mol^{-1}·K^{-1})	$\Delta_{ads}G^0$ at 298 K (kJ·mol^{-1})
Site 1	−26.5	337.8	−127.2
Site 2	−126.9	0.50	−127.0

The standard enthalpy of adsorption onto POS-50 was strongly negative for both adsorption sites. The enthalpic contribution to the standard Gibbs free energy mainly comes from hydrogen bonding between hydroxy and carboxy functional surface groups of POS-50 and OTC molecules. Upon adsorption, these hydrogen bonds formed induce at the same time the broken of hydrogen bonds between water and both OTC. $\Delta_{ads}H^0$ is the balance of all these processes. The exothermic balance for adsorption to POS-50 reveals that hydrogen bonds between OTC and surface hydroxyl are stronger. This is the result of POS-50 hydroxyl groups interacting more favorably with OTC. $\Delta_{ads}S^0$ is positive for both the two sites adsorption processes. Thus, $\Delta_{ads}H^0$ = −26.5 kJ·mol^{-1} and $\Delta_{ads}S^0$ = 337.8 J·mol^{-1}·K^{-1} for the adsorption site onto POS-50; and $\Delta_{ads}H^0$ = −126.8 kJ·mol^{-1} and $\Delta_{ads}S^0$ = 0.5 J·mol^{-1}·K^{-1}

for the site adsorption off the biomaterial. For both sites, the entropic contribution ($-T\,\Delta_{ads}S^0$) to the standard Gibbs free energy is lower than the enthalpic contribution, so that $\Delta_{ads}G^0$ assumes a negative value.

The standard enthalpy of site 2 adsorption off phenolic sites was strongly negative. Such an exothermic adsorption process suggests the formation of strong hydrogen bonds between OTC and phenolic groups. The site 1 adsorption onto POS-50 material is much less exothermic. The hydrogen bonds between OTC and the primary hydroxyl groups of monosaccharides are expected to be weaker in the adsorption process at Site 1. In addition, this decrease in the exothermic process results from compensation of the exo- and endothermic processes, to know the adsorption of one OTC molecule results in the release of many water molecules, so that the net balance is an increase of the number of free molecules. However, although the OTC molecules adsorbed off the adsorption sites are non-located and mobile, the adsorption to biomass material is localized. As a result, the entropy for adsorption off POS-50 is higher.

3.2.4. Kinetics of adsorption

In applications to analysis such as liquid chromatographic separations and sample pre-concentration in solid phase extraction devices (SPME), the kinetics of adsorption is extremely important. Fast adsorption provides for a high flow rate and a fast analysis time. Pre-concentration using SPME necessitates that almost all of the analyte be absorbed during the residence time in the SPME cartridge. The influence of contact time on OTC adsorption onto POS-50, POS-75, POS-100 and POS-fiber at different concentrations of OTC (from 5 10^{-5} to 10^{-4} mol·L^{-1}) was studied using the depletion method (Fig. 10). The adsorption of OTC onto POS-50 material was much larger than onto others tested materials during the adsorption equilibration time. At all tested OTC concentrations, binding to Posidonia biomaterials were quite fast processes. Adsorption equilibrium was reached within the first few minutes. 90 % uptake of OTC onto POS-50 occurred within 10 min. A typical time scale taken from the scarce experimental data is about 15 min using activated in alkaline medium and functionalized Posidonia materials (Boubakri et al. 2017). Theoretical studies were established to explain the nature of adsorption.

The nonlinear forms of the pseudo-first order model and pseudo-second order:

$$Q_t = Q_e - Q_e e^{-k_1 t} \qquad \text{(Eq 12)}$$

$$Q_t = \frac{k_2 {Q_e}^2 t}{1 + k_2 Q_e t} \qquad \text{(Eq 13)}$$

where k_1 (min^{-1}) et k_2 (mg·g^{-1}·min^{-1}) are the pseudo-first order and pseudo-second order kinetic constants, respectively. Q_e and Q_t are the quantities of OTC (mg·g^{-1}) adsorbed at equilibrium and at time t.

In order to determine the model of the adsorption kinetics, it is required to compare the value of Q_e calculated by the theoretical equation with that of the experimental value (Lin and Wang 2009). Table 6 groups the coefficients

of the equations obtained by considering a pseudo-first order or pseudo-second order kinetics for Posidonia biomaterials. It can be seen from this table that the values of the quantities adsorbed at equilibrium for all concentrations calculated by the equation of the pseudo-second order model are close to the values measured experimentally. It can be also seen that increasing the initial OTC concentration results in an increase in the adsorption capacity but the rate constant remains constant. The initial number of sites being the same, the competition on these sites becomes more and more important as the concentration of OTC increases. In addition, the average relative error (*ARE*, Eq 8) of the pseudo-second order model are small and lower than those obtained with the pseudo-first order model. At the same time, Fig. 10 clearly shows that the pseudo-second order kinetic model fits perfectly to the experimental data. According to comparable instances reported in the literature on various types of pollutants (organic and inorganic substances), the pseudo-second order kinetic model has commonly been used to describe adsorption processes (Febrianto et al. 2009; Anirudhan and Suchithra 2010; Bhatnagar and Sillanpää 2010; Miranda et al. 2014).

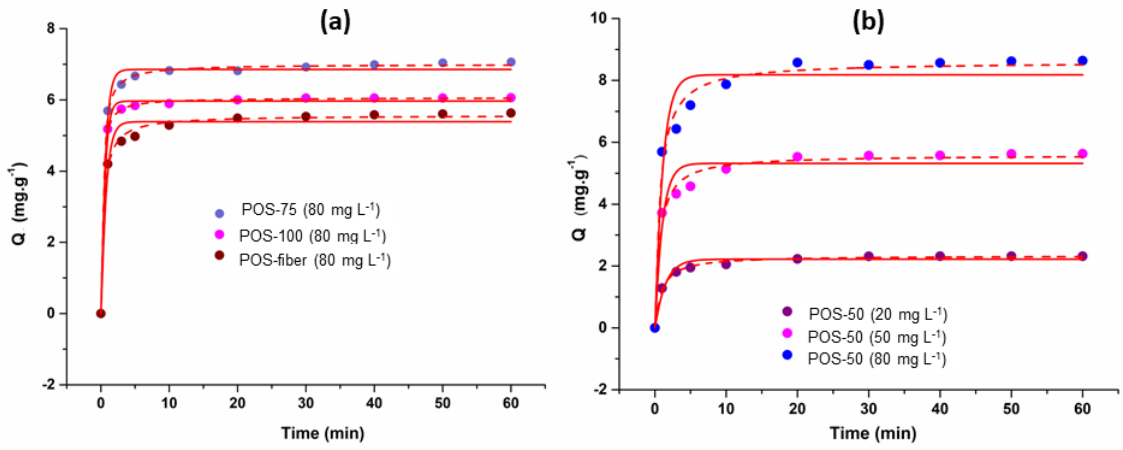

Figure 10. Experimental data of adsorption kinetics and nonlinear fits of the pseudo-first-order (red dashed lines) and pseudo-second-order (red solid lines) models for corresponding adsorption of OTC to (a): POS-75, POS-100 and POS-fiber at 20 mg·L^{-1} and (b): POS-50 at initial concentration 20 mg·L^{-1}, 50 mg·L^{-1} and 80 mg·L^{-1}.

Table 6. Kinetic parameters of the pseudo-first order and pseudo-second order models of the adsorption study of OTC onto POS-50, POS-75, POS-100 and POS-fiber biomaterials.

Posidonia biomaterials	C_0 (mg·L^{-1})	$Q_{e,exp}$ (mg·g^{-1})	**Pseudo-first-order model**			**Pseudo-second-order model**		
			k_1 (min^{-1})	$Q_{e,calc}$ (mg·g^{-1})	*ARE*	k_2 (g·mg^{-1}·min^{-1})	$Q_{e,calc}$ (mg·g^{-1})	*ARE*
POS-50	20	2.32	1.75	2.22	0.107	0.49	2.33	0.020
	50	5.63	1.76	5.32	0.162	0.50	5.58	0.047
	80	8.64	1.70	8.18	0.164	0.50	8.59	0.031
POS-75	80	7.04	1.42	6.85	0.060	0.40	7.00	0.031
POS-100	80	6.05	1.45	5.97	0.039	0.43	6.06	0.011
POS-fiber	80	5.63	1.45	5.39	0.097	0.49	5.57	0.048

3.3. Comparative study

The adsorption capacities and the equilibrium time of Posidonia biomaterial with respect to OTC have been compared to some recently reported sorbents. The adsorption capacity of Posidonia is comparable to that of the majority of these adsorbents, which are therefore suitable for the removal of OTC from wastewater (Harja and Ciobanu 2018, Minale et al. 2021, Pham et al. 2019, Wu et al. 2018). Considering the difference in physical properties of adsorbents and experimental conditions, an accurate evaluation using adsorption capacity and contact time data is quite difficult to make, although our data still provide useful information at least on the order of magnitude. Finally, due to the relatively low raw material cost and fast adsorption time, Posidonia particles have the potential to be cost effective adsorbents for the removal of OTC from aqueous solutions and a good candidate towards the environment.

4. Conclusion

Results highlighted that the Posidonia biomaterial exhibit a good ability and efficient uptake of oxytetracycline antibiotics from aqueous solutions, due to the fact that Posidonia has more than 80% organic compounds and functional surface which could be uptake sites. Different adsorption process, such as solution pH, contact time, initial OTC concentration, and temperature have been studied and optimized. The optimal removal occurred at pH 6.0. A correct thermodynamic approach taking into account the presence of two types of adsorption sites has been applied using the bi-Langmuir adsorption isotherm better than the simpler Langmuir isotherm that considers a localized adsorption on one single type of site. The thermodynamic study under variation of the temperature shows that interactions are of entropic nature, which is expected for a cation exchange phenomenon driven by electrostatic interactions. The kinetic equilibrium was rapidly established in about 10 min. The quite fast kinetics of adsorption makes the POS-50 a sorbent material able to extract a high capacity of OTC from aqueous media in the framework of an application to SPME. The experimental data were closely fitted to the pseudo-second-order model, suggesting that chemisorption is predominant. These promising results show the successful use of native Posidonia as an adsorbent medium to remove organic micro-contaminants from wastewater. It is inexpensive and can also contribute to a circular economy as it is made of pellets washed up on sea beaches. The results could be useful to implement the large-scale use of Posidonia as material adsorbing organic pollutants in the treatment of contaminated water.

Acknowledgments
This work was supported by the Cross-border project Italy-Tunisia "Méthodologies d'Économie Durable pour les Déchets Côtiers Utilisables des Plages" (MEDDé.Co.U.Plages IS_3.2_086).

Statements and Declarations
- **Ethical Approval**: Not applicable
- **Consent to Participate**: Not applicable
- **Consent to Publish**: Not applicable
- **Funding**: The authors declare that no funds, grants, or other support were received during the preparation of this manuscript.
- **Competing Interests**: All the authors (Karima Ferchichi, Noureddine Amdouni, Yves Chevalier and Souhaira Hbaieb) declare that they have no known competing financial or no financial interests or personal relationships which have or could be perceived to have influenced the work reported in this article.
- **Author contributions**: All authors contributed to the study conception and design. Material preparation, data collection and analysis were performed by Karima Ferchichi, Noureddine Amdouni, Yves Chevalier and Souhaira Hbaieb. The first draft of the manuscript was written by [Karima Ferchichi] and all authors commented on previous versions of the manuscript. All authors read and approved the final manuscript.
- **Availability of data and materials**: All authors declare that all data and materials of their published claims comply with field standards.

References

Aghababaei A, Ncibi MC, Sillanpää M (2017) Optimized removal of Oxytetracycline and cadmium from contaminated waters using chemically-activated and pyrolyzed biochars from forest and wood-processing residues. Bioresour Technol 239:28–36. doi:10.1016/j.biortech.2017.04.119

Anirudhan TS, Suchithra PS (2010) Heavy metals uptake from aqueous solutions and industrial wastewaters by humic acid-immobilized polymer/bentonite composite: Kinetics and equilibrium modeling Chem Eng J 156:146–156. doi:10.1016/j.cej.2009.10.011

Astudillo-Pascual M, Domínguez I, Aguilera PA, Garrido Frenich A (2021) New phenolic compounds in Posidonia Oceanica seagrass: A comprehensive array using high resolution mass spectrometry. Plants 10:864. doi:10.3390/plants10050864

Ayadi C, Anene A, Kalfat R, Chevalier Y, Hbaieb S (2020) Molecular imprints frozen by strong intermolecular interactions in place of cross-linking. Chem Eur J 27:2175–2183. doi:10.1002/chem.202004580

Ayadi C, Anene A, Kalfat R, Chevalier Y, Hbaieb S (2019) Molecularly imprinted polyaniline on silica support for the selective adsorption of benzophenone-4 from aqueous media. Colloids Surf A: Physicochem Eng Asp 567:32–42. doi:10.1016/j.colsurfa.2019.01.042

Banhishikha D, Moumita M, Mahashweta B, Kartick LB, Animesh D, Dijendra NR (2020) The effective adsorption of tetracycline onto zirconia nanoparticles synthesized by novel microbial green technology. J Environ Manag 261:110235. doi:10.1016/j.jenvman.2020.110235

Bhatnagar A, Sillanpää M (2010) Utilization of agro-industrial and municipal waste materials as potential adsorbents for water treatment—A review. Chem Eng J 157:277–296. doi:10.1016/j.cej.2010.01.007

Ben Douissa N, Dridi-Dhaouadi S, Mhenni MF (2016) Spectrophotometric investigation of the interactions between cationic (C.I. Basic Blue 9) and anionic (C.I. Acid Blue 25) dyes in adsorption onto extracted cellulose from Posidonia oceanic in single and binary system. Water Sci Technol 73:2211–2221. doi:10.2166/wst.2016.068

Boehm HP (2002) Surface oxides on carbon and their analysis: a critical assessment. Carbon 40:145–149. doi:10.1016/s0008-6223(01)00165-8

Boni MR, Marzeddu S, Tatti F, Raboni M, Mancini G, Luciano A, Viotti P (2021) Experimental and numerical study of biochar fixed bed column for the adsorption of arsenic from aqueous solutions. Water 13:915. doi:10.3390/w13070915

Boubakri S, Djebbi MA, Bouaziz Z, Namour P, Ben Haj Amara A, Ghorbel-Abid I, Kalfat R (2017) Nanoscale zero-valent iron functionalized Posidonia Oceanica marine biomass for heavy metal removal from water. Environ Sci Pollut Res 24:27879–27896. doi:10.1007/s11356-017-0247-0

Chadlia A, Farouk MM (2010) Chemical modification of Posidonia with cyclic anhydrides: effect on thermal stability. Carbohydr Res 345:264–269. doi:10.1016/j.carres.2009.11.006

Cheng N, Wang B, Wu P, Lee X, Xing Y, Chen, M, Gao B (2021) Adsorption of emerging contaminants from water and wastewater by modified biochar: A review. Environ Pollut 273:116448. doi:10.1016/j.envpol.2021.116448

Chenguang L, Qian T, Yanlei Z, Yuanyuan L, Xiaoman Y, Hao Z, Lingyun C, Fengmin L (2022) Sequential combination of photocatalysis and microalgae technology for promoting the degradation and detoxification of typical antibiotics. Water Res 210:117985. doi:10.1016/j.watres.2021.117985

Coletti A, Valerio A, Vismara E (2013) Posidonia Oceanica as a renewable lignocellulosic biomass for the synthesis of cellulose acetate and glycidyl methacrylate grafted cellulose. Mater 6:2043–2058. doi:10.3390/ma6052043

De Gisi S, Lofrano G, Grassi M, Notarnicola M (2016) Characteristics and adsorption capacities of low-cost sorbents for wastewater treatment. A review Sustain Mater Technol 9:10–40. doi:10.1016/j.susmat.2016.06.002

De Leon-Condes C, Barrera-Diaz C, Barrios J, Becerril E, Reyes-Perez H (2017) A coupled ozonation-electrooxidation treatment for removal of bisphenol A, nonylphenol and triclosan from wastewater sludge. Int J Environ Sci Technol 14:707–716. doi:10.1007/s13762-016-1178-x

Décima MA, Marzeddu S, Barchiesi M, Di Marcantonio C, Chiavola A, Boni MR (2021) A Review on the removal of carbamazepine from aqueous solution by using activated carbon and biochar. Sustainability 13:11760. doi:10.3390/su132111760

Donut N, Cavas L (2017) Artificial neural network modeling of tetracycline biosorption by pre-treated Posidonia Oceanica. Turkish J Fish Aquat Sci 17:1317–1333. doi:10.4194/1303-2712-v17_6_50

Dos Santos AJ, Kronka MS, Fortunato GV, Lanza MRV (2021) Recent advances in electrochemical water technologies for the treatment of antibiotics: A short review. Curr Opin Electrochem 26:100674. doi:10.1016/j.coelec.2020.100674

Douissa NB, Bergaoui L, Mansouri S, Khiari R, Mhenni MF (2013) Macroscopic and microscopic studies of methylene blue sorption onto extracted celluloses from Posidonia Oceanica. Ind Crops Prod 45:106–113. doi:10.1016/j.indcrop.2012.12.007

Dutta J, Mala AA (2020) Removal of antibiotic from the water environment by the adsorption technologies: A review. Water Sci Technol 82:401–426. doi:10.2166/wst.2020.335

El Achaby M, Fayoud N, Figueroa-Espinoza MC, Ben Youcef H, Aboulkas A (2018) New highly hydrated cellulose microfibrils with a tendril helical morphology extracted from agro-waste material: application to removal of dyes from waste water. RSC Adv 8:5212–5224. doi:10.1039/c7ra10239a

Elmorsi RR, El-Wakeel ST, Shehab El-Dein WA, Lotfy HR, Rashwan WE, Nagah M, Abou-El-Sherbini KS (2019) Adsorption of methylene blue and Pb^{2+} by using acid-activated Posidonia Oceanica waste. Sci Rep 9:1–12. doi:10.1038/s41598-019-39945-1

Fanourakis SK, Peña-Bahamonde J, Bandara PC, Rodrigues DF (2020) Nano-based adsorbent and photocatalyst use for pharmaceutical contaminant removal during indirect potable water reuse. npj Clean Water 3:1–15. doi:10.1038/s41545-019-0048-8

Febrianto J, Kosasih AN, Sunarso J, Ju YH, Indraswati N, Ismadji S (2009) Equilibrium and kinetic studies in adsorption of heavy metals using biosorbent: A summary of recent studies. J Hazard Mater 162:616–645. doi:10.1016/j.jhazmat.2008.06.042

Fornstedt T, Forssén P, Samuelsson J (2013) Modeling of preparative liquid chromatography. J Liq Chromatogr 407–425. doi:10.1016/b978-0-12-415807-8.00018-3

Gaspard S, Altenor S, Dawson EA, Barnes PA, Ouensanga A (2007) Activated carbon from vetiver roots: gas and liquid adsorption studies. J Hazard Mater 144:73–80. doi:10.1016/j.jhazmat.2006.09.089

Geetha G, Sruthi AA, Chandrasekaran N, Amitava M (2020) A review on tetracycline removal from aqueous systems by advanced treatment techniques. RSC Adv 10:27081–27095. doi:10.1039/D0RA04264A

Gupta G, Khan J, Singh NK (2021) Application and efficacy of low-cost adsorbents for metal removal from contaminated water. Mater Today 43:2958–2964. doi:10.1016/j.matpr.2021.01.002

Haddar M, Elloumi A, Koubaa A, Bradai C, Migneault S, Elhalouani F (2018) Synergetic effect of Posidonia Oceanica fibres and deinking paper sludge on the thermo-mechanical properties of high density polyethylene composites. Ind Crops Prod 121: 26–35. doi:10.1016/j.indcrop.2018.04.075

Han B, Weatherley AJ, Mumford K, Bolan N, He J-Z, Stevens GW, Chen D (2022) Modification of naturally abundant resources for remediation of potentially toxic elements: A review. J Hazard Mater 421:126755. doi:10.1016/j.jhazmat.2021.126755

Harja M, Ciobanu G (2018) Studies on adsorption of oxytetracycline from aqueous solutions onto hydroxyapatite. Sci Total Environ 628-629:36–43. doi:10.1016/j.scitotenv.2018.02.027

Hembach N, Alexander J, Hiller C, Wieland A, Schwartz T (2019) Dissemination prevention of antibiotic resistant and facultative pathogenic bacteria by ultrafiltration and ozone treatment at an urban wastewater treatment plant. Sci Rep 9:12843. doi:10.1038/s41598-019-49263-1

Hussain Z, Chang N, Sun J, Xiang S, Ayaz T, Zhang H, Wang H (2022) Modification of coal fly ash and its use as low-cost adsorbent for the removal of directive, acid and reactive dyes. J Hazard Mater 422:126778. doi:10.1016/j.jhazmat.2021.126778

Langmuir I (1918) The adsorption of gases on plane surfaces of glass, mica and platinum. J Am Chem Soc 40:1361–1403. doi:10.1021/ja02242a004

Lin J, Wang L (2009) Comparison between linear and non-linear forms of pseudo-first-order and pseudo-second-order adsorption kinetic models for the removal of methylene blue by activated carbon. Front Environ Sci Eng China 3:320–324. doi:10.1007/s11783-009-0030-7

Liu L, Luo XB, Ding L, Luo SL (2019) Application of nanotechnology in the removal of heavy metal from water. In: Luo X, Deng F (ed) Micro and Nano Technologies, Nanomaterials for the Removal of Pollutants and Resource Reutilization, 1st edn. Elsevier, 83–147 doi:10.1016/b978-0-12-814837-2.00004-4

Liu X, Huang D, Lai C, Zeng G, Qin L, Zhang C, Yi H, Li B, Deng R, Liu S, Zhang Y (2018) Recent advances in sensors for tetracycline antibiotics and their applications, Trends Anal Chem 109:260–274. doi:10.1016/j.trac.2018.10.011

Lu TH, Chen CY, Wang WM, Liao C-M (2021) A risk-based approach for managing aquaculture used oxytetracycline-induced TetR in surface water across Taiwan regions. Front Pharmacol 12:1–15. doi:10.3389/fphar.2021.803499

Ma T, Chen L, Wu L, Christie P, Luo Y (2016) Toxicity of OTC to Ipomoea aquatica Forsk and to microorganisms in a long-term sewage-irrigated farmland soil. Environ Sci Pollut Res 23:15101–15110. doi:10.1007/s11356-016-6644-y

Maisano S, Urbani F, Cipitì F, Freni F, Chiodo V (2019) Syngas production by BFB gasification: Experimental comparison of different biomasses. Int J Hydrog Energy 44:4414-4422. doi:10.1016/j.ijhydene.2018.11.148

Meseguer VF, OrtuñoJF, Aguilar MI, Pinzón-Bedoya ML, Lloréns M, Sáez J, Pérez-Marín AB (2016) Biosorption of cadmium(II) from aqueous solutions by natural and modified non-living leaves of Posidonia Oceanica. Environ Sci Pollut Res 23: 24032–24046. doi:10.1007/s11356-016-7625-x

Minale M, Guadie A, Li Y, Meng Y, Wang X, Zhao J (2021) Enhanced removal of oxytetracycline antibiotics from water using manganese dioxide impregnated hydrogel composite: Adsorption behavior and oxidative degradation pathways. Chemosphere 280:130926. doi:10.1016/j.chemosphere.2021.130926

Miranda LDL, Bellato CR, Fontes MPF, de Almeida MF, Milagres JL, Minim LA (2014) Preparation and evaluation of hydrotalcite-iron oxide magnetic organocomposite intercalated with surfactants for cationic methylene blue dye removal. Chem Eng J 254:88–97. doi:10.1016/j.cej.2014.05.094

Normah N, Juleanti N, Palapa NR, Taher T, Siregar PMSBN, Wijaya A, Lesbani A (2022) Hydrothermal carbonization of rambutan peel (Nephelium lappaceum L.) as a green and low-cost adsorbent for Fe(II) removal from aqueous solutions. J Chem Ecol 38:284–300. doi:10.1080/02757540.2022.2040996

Nowicki P, Kazmierczak J, Pietrzak R (2015) Comparison of physicochemical and sorption properties of activated carbons prepared by physical and chemical activation of cherry stones. Powder Technol 269:312–319. doi:10.1016/j.powtec.2014.09.023

Pennesi C, Totti C, Beolchini F (2013) Removal of vanadium(III) and molybdenum(V) from wastewater using Posidonia Oceanica (Tracheophyta) biomass. PLoS One 8:e76870. doi:10.1371/journal.pone.0076870

Pham TD, Tran TT, Le VA, Pham TT, Dao TH, Le TS (2019) Adsorption characteristics of molecular oxytetracycline onto alumina particles: The role of surface modification with an anionic surfactant. J Mol Liq 287:110900. doi:10.1016/j.molliq.2019.110900

Plis A, Lasek JA, Zuwała J, Yu CC, Iluk A (2016) Combustion performance evaluation of Posidonia Oceanica using TGA and bubbling fluidized-bed combustor (batch reactor). J Sustain Min 15:181–190. doi:10.1016/j.jsm.2017.03.006

Plis A, Lasek J, Skawinska A, Kopczynski M (2014) Thermo-chemical properties of biomass from Posidonia Oceanica. Chem Pap 68:879–889. doi:10.2478/s11696-013-0532-4

Prarat P, Hongsawat P, Punyapalakul P (2020) Amino-functionalized mesoporous silica-magnetic graphene oxide nanocomposites as water-dispersible adsorbents for the removal of the oxytetracycline antibiotic from aqueous solutions: adsorption performance, effects of coexisting ions, and natural organic matter. Environ Sci Pollut Res 27:6560–6576. doi:10.1007/s11356-019-07186-4

Punamiya P, Sarkar D, Rakshit S, Datta R (2013) Effectiveness of aluminum-based drinking water treatment residuals as a novel sorbent to remove tetracyclines from aqueous medium. J Environ Qual 42:1449–1459. doi:10.2134/jeq2013.03.0082

Radhakrishnan S, Nagarajan S, Belaid H, Farha C, Iatsunskyi I, Coy E, Bechelany M (2021) Fabrication of 3D printed antimicrobial polycaprolactone scaffolds for tissue engineering applications. Mater Sci Eng C 118:111525. doi:10.1016/j.msec.2020.111525

Rahmani AR, Nematollahi D, Samarghandi MR, Samadi MT, Azarian G (2018) A combined advanced oxidation process: electrooxidation-ozonation for antibiotic ciprofloxacin removal from aqueous solution. J Electroanal Chem 808:82–89. doi:10.1016/j.jelechem.2017.11.067

Ribeiro AR, Sures B, Schmidt TC (2018) Cephalosporin antibiotics in the aquatic environment: A critical review of occurrence, fate, ecotoxicity and removal technologies. Environ Pollut 241:1153–1166. doi:10.1016/j.envpol.2018.06.040

Stavropoulos GG, Zabaniotou AA (2005) Production and characterization of activated carbons from olive-seed waste residue. Micropor Mesopor Mater 82:79–85. doi:10.1016/j.micromeso.2005.03.009

Tarchoun AF, Trache D, Klapötke TM (2019) Microcrystalline cellulose from Posidonia Oceanica brown algae: Extraction and characterization. Int J Biol Macromol 138:837–845. doi:10.1016/j.ijbiomac.2019.07.176

Saleh AT, Mustaqeem M, Khaled M (2022) Water treatment technologies in removing heavy metal ions from wastewater: A review. Environ Nanotechnol Monit Manag 17:100617. doi:10.1016/j.enmm.2021.100617

Qin W, Xiangcao L, Ke Y, Shaojing Z, Shaohua Z, Benhua W, Jianing Y, Yi Z, Xiangzhi S, Minhuan L (2022) Carbon dots and Eu^{3+} hybrid-based ratiometric fluorescent probe for oxytetracycline detection. Ind Eng Chem Res 61:5825–5832. doi:10.1021/acs.iecr.2c00307

Wang B, Gao B, Fang J (2018) Recent advances in engineered biochar productions and applications. Crit Rev Environ Sci Technol 47:2158–2207. doi:10.1080/10643389.2017.1418580

Wohlert M, Benselfelt T, Wågberg L, Furó I, Berglund L A, Wohlert J (2022) Cellulose and the role of hydrogen bonds: not in charge of everything. Cellulose 29:1–23. doi:10.1007/s10570-021-04325-4

Wu Y, Yue Q, Gao Y, Ren Z, Gao B (2018) Performance of bimetallic nanoscale zero-valent iron particles for removal of oxytetracycline. J Environ Sci 69:173–182. doi:10.1016/j.jes.2017.10.006

Zaafouri K, Ben Hassen Trabelsi A, Krichah S, Ouerghi A, Aydi A, Claumann CA, Wüst ZA, Naoui S, Bergaoui L, Hamdi M (2016) Enhancement of biofuels production by means of co-pyrolysis of Posidonia Oceanica (L.) and frying oil wastes: Experimental study and process modeling. Bioresource Technol 207:387–398. doi:10.1016/j.biortech.2016.02.004

Zeidman AB, Rodriguez-Narvaez OM, Moon J, Bandala ER (2020) Removal of antibiotics in aqueous phase using silica-based immobilized nanomaterials: A review. Environ Technol Innov 20:101030. doi:10.1016/j.eti.2020.101030

Zhao N, Wang Y, Hou S, Zhao L (2020) Functionalized carbon quantum dots as fluorescent nanoprobe for determination of tetracyclines and cell imaging, Microchim Acta 187–351. doi:10.1007/s00604-020-04328-1